ORGANOMETALLICS

pubs.acs.org/Organometallics Article

Reactions of Triisobutylaluminum with Unbridged or Bridged Group IV Metallocene Dichlorides

Damien B. Culver, Jamesjohn Corieri, Graham Lief,* and Matthew P. Conley*

Cite This: *Organometallics* 2022, 41, 892−899 Read Online

ACCESS | Metrics & More | Article Recommendations | Supporting Information

Downloaded via UNIV OF CALIFORNIA RIVERSIDE on June 4, 2024 at 20:01:14 (UTC).
See https://pubs.acs.org/sharingguidelines for options on how to legitimately share published articles.

ABSTRACT: Reactions between zirconocene or hafnocene dichlorides and alkylaluminum activators are involved in several catalytic reactions. This study describes the products formed in reactions between unbridged metallocenes with varying steric profiles (Cp_2ZrCl_2 (**1**), Cp_2HfCl_2 (**2**), $Cp^*CpZrCl_2$ (**3**), $Cp^*_2ZrCl_2$ (**4**), $Cp^*_2HfCl_2$ (**5**)) or *ansa*-zirconocenes (*rac*-(2-methyl-SBI)-$ZrCl_2$ (**6**), and *rac*-(EBI)$ZrCl_2$ (**7**); 2-methyl-SBI = *rac*-Me_2Si(2-methyl-indenyl)$_2$; *rac*-EBI = *rac*-C_2H_4(indenyl)$_2$) with 12 equiv of triisobutylaluminum (TIBA). A 12:1 Al/Zr ratio was chosen because previous results (*ACS Cent Sci.* **2021**, *7*, 1225−1231) showed that an unbridged metallocene reacted with 12 equiv of TIBA to form mixtures of bridging metal hydrides in solution. This study shows that sterically open, unbridged metallocenes generate similar reaction products, but sterically crowded metallocenes do not react with TIBA. *Rac*-(EBI)$ZrCl_2$ reacts with 12 equiv of TIBA to form a mixture of *rac*-(EBI)Zr($CH_2CH(CH_3)_2$)Cl (**7a**, major, ∼95%) and *rac*-(EBI)Zr(μ-Cl)(μ-CH_2CH_2)Al^iBu_2 (**7b**, minor, ∼5%) after ∼10 min at room temperature. This mixture evolves over the course of ∼2 days to form *rac*-(EBI)Zr(μ-H)(μ-CH_2CH_2)Al^iBu_2 (**7c**), *rac*-(EBI)ZrH(μ-H)$_2$Al^iBu_2 (**7d**), *rac*-(EBI)ZrH(μ-H)$_2$[μ-H(Al^iBu_2)$_2$] (**7e**), and *rac*-(EBI)ZrH(μ-H)$_2$[μ-Cl(AliBu_2)$_2$] (**7f**). However, **6** reacts with TIBA to form *rac*-(2-methyl-SBI)Zr($CH_2CH(CH_3)_2$)Cl (**6a**) as the only product.

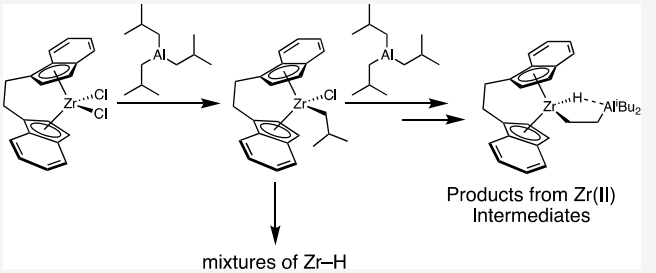

INTRODUCTION

The chemical steps involved in catalyst activation determine reactivity and selectivity patterns. Group IV metallocenes are excellent representative examples showing how subtle changes in catalyst activation result in divergent reactivity; representative examples are summarized in Figure 1. Alkylation of Cp_2ZrCl_2 (Cp = cyclopentadienyl) with *n*-BuLi transiently forms $Cp_2Zr(n\text{-Bu})_2$ that eliminates butane to form Cp_2Zr(1-butene);[1] this compound behaves like Cp_2Zr and has numerous applications in organic synthesis.[2] $AlMe_3$ reacts with Cp_2ZrCl_2 to form $Cp_2ZrCl(\mu\text{-Me})(\mu\text{-Cl})AlMe_2$.[3] The reactivity of $Cp_2ZrCl(\mu\text{-Me})(\mu\text{-Cl})AlMe_2$ in carboalumination reactions is probably related to the formation of [Cp_2ZrMe]-[Cl_2AlMe_2];[4] related intermediates were originally proposed by Breslow as active species in ethylene polymerization reactions mediated by Cp_2TiCl_2 and $ClAlEt_2$.[5] However, $AlEt_3$ results in entirely different reaction products. Kaminsky showed that $AlEt_3$ reacts with Cp_2ZrCl_2 to form $Cp_2Zr(\mu\text{-Cl})(\mu\text{-}CH_2CH(AlEt_2)_2)$.[6] Similar species were isolated in solvolysis reactions of Cp_2ZrMe_2 and $AlMe_3$ containing small amounts of $EtAlMe_2$.[7]

Partial hydrolysis of $AlMe_3$ yields methylaluminoxane (MAO),[8] which reacts with Cp_2ZrCl_2 to form [Cp_2ZrMe]-[MeMAO] ion pairs.[9] Free $AlMe_3$ coordinates to the metallocenium ion to generate bridging [$Cp_2Zr(\mu\text{-Me})_2AlMe_2$]$^+$.[10] The reaction sequence to generate these species involves transmetallation between Zr and Al, followed

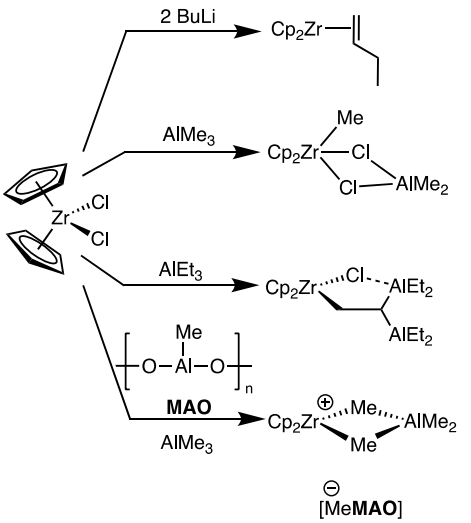

Figure 1. Representative reactions of Cp_2ZrCl_2 with alkylaluminum reagents.

Received: February 4, 2022
Published: April 1, 2022

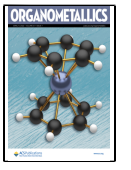

© 2022 American Chemical Society

https://doi.org/10.1021/acs.organomet.2c00067
Organometallics 2022, 41, 892−899

by abstraction of Zr−Me groups by Lewis acidic Al sites present on the amorphous MAO surface. Related species form as discrete ion pairs in reactions of Cp_2ZrMe_2, $[CPh_3][B(C_5F_5)_4]$, and $AlMe_3$ to form $[Cp_2Zr(\mu\text{-}Me)_2AlMe_2][B(C_5F_5)_4]$.[11] Derivates of these metallocenium ion pairs are catalysts in carboalumination reactions[12] and are very active olefin polymerization catalysts.[13]

Triisobutylaluminum (TIBA) promotes interesting reactivity trends in catalytic mixtures containing zirconocenes, suggesting different reaction pathways than those shown in Figure 1. Addition of TIBA to zirconocene/MAO mixtures increases the polymer molecular weight compared to $AlMe_3$ or $AlEt_3$ additives.[14] The origin of this behavior is not clear but may be related to slow Zr−R^+/Al−^{i}Bu chain transfer kinetics or incorporation of Al−^{i}Bu groups into the MAO framework.[15] However, TIBA also facilitates the formation of Zr−H^+ species under polymerization conditions.[16] Formation of group IV hydrides in the presence of TIBA appears to be somewhat general. Organozirconium species supported on silica-alumina formally activate C−C bonds in the presence of TIBA by forming hydrides,[17] and $Cp^b_2ZrCl_2$ (Cp^b = 1-butylcyclopentadienyl) reacts with Al^iBu_3 (Al/Zr = 12) to form mixtures of $Cp^b_2Zr(\mu\text{-}H)_3(Al^iBu_2)Al^iBu_3$ (**A**) and $Cp^b_2Zr(\mu\text{-}H)_3(Al^iBu_2)_3(\mu\text{-}Cl)_2$ (**B**), eq 1.[18] Clean generation of **A** is

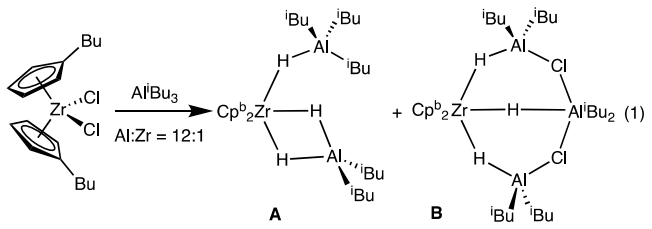

possible using the chloride-free synthesis from $[Cp^b_2ZrH_2]_2$ in the presence of stoichiometric TIBA and HAl^iBu_2. **B** forms as the sole product in reactions of $Cp^b_2ZrCl_2$ with HAl^iBu_2.[19] However, $Ph_2C(CpFlu)ZrCl_2$ reacts with excess TIBA to form $Ph_2C(CpFlu)Zr(^i Bu)Cl$, independent of the Al/Zr ratio.[20] The reaction between Cp_2ZrCl_2 and excess Al^iBu_3 was proposed to form $[Cp_2ZrH_2]_2{*}(Al^iBu_3)_2$,[20,21] but the available ^{1}H NMR data appear consistent with the formation of species similar to **B**.[19]

This paper describes the reaction of metallocenes shown in Figure 2 with excess TIBA. The metallocenes include sterically

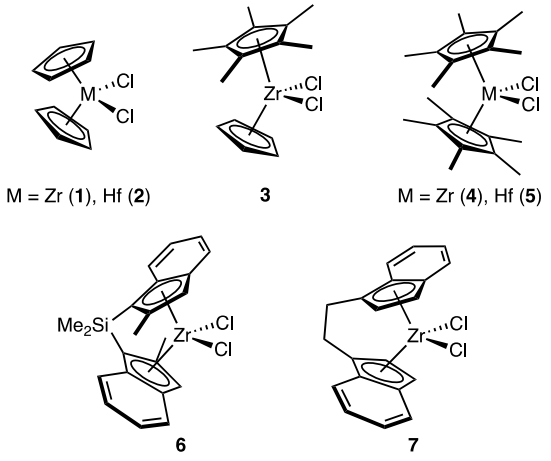

Figure 2. Metallocenes studied in the presence of excess TIBA.

open unbridged metallocenes such as Cp_2ZrCl_2 (**1**) and Cp_2HfCl_2 (**2**) and more sterically congested $Cp^*CpZrCl_2$ (**3**), $Cp^*_2ZrCl_2$ (**4**), and $Cp^*_2HfCl_2$ (**5**) to probe the efficiency of this reaction as the steric environment is modified. Precatalysts **6** and **7** are common *ansa*-metallocenes used in polymerization reactions.

RESULTS AND DISCUSSION

Unbridged Metallocenes. **1** reacts with excess TIBA (Al/Zr = 12:1) to from a mixture of $Cp_2Zr(\mu\text{-}H)_3(Al^iBu_2)Al^iBu_3$ (**1a**), $Cp_2Zr(\mu\text{-}H)_3(Al^iBu_2)_3(\mu\text{-}Cl)_2$ (**1b**), and isobutene. **2** and **3** also generate similar mixtures of **2a**/**b** and **3a**/**b**. Relevant ^{1}H NMR data of the hydrides formed in solution for these species are given in Table 1. The variable temperature ^{1}H NMR data

Table 1. Selected ^{1}H NMR Signals for Reactions of Unbridged Metallocenes with TIBA (Al/Zr = 12:1)[a]

	Zr−H	ligand
$Cp_2Zr(\mu\text{-}H)_3(Al^iBu_2)Al^iBu_3$ (**1a**)	−1.22 (d, 1H, J_{HH} = 8.2 Hz)	5.48 (s, 10 H)
	−1.90 (d, 1H, J_{HH} = 8.0 Hz)	
	−2.53 (br, 1H)	
$Cp_2Zr(\mu\text{-}H)_3(Al^iBu_2)_3(\mu\text{-}Cl)_2$ (**1b**)	−1.16 (t, 1H, J_{HH} = 7.4 Hz)	5.47 (s, 10H)
	−2.55 (d, 2H, J_{HH} = 7.3 Hz)	
$Cp_2Hf(\mu\text{-}H)_3(Al^iBu_2)Al^iBu_3$ (**2a**)	−0.49 (d, 1H, J_{HH} = 9.1 Hz)	5.48 (s, 10 H)
	−0.55 (d, 1H, J_{HH} = 9.5 Hz)	
	−1.73 (br, 1H)	
$Cp_2Hf(\mu\text{-}H)_3(Al^iBu_2)_3(\mu\text{-}Cl)_2$ (**2b**)	−0.45 (t, 1H, J_{HH} = 6.1 Hz)	5.47 (s, 10 H)
	−1.65 (br, 1H)	
$Cp^*CpZr(\mu\text{-}H)_3(Al^iBu_2)Al^iBu_3$ (**3a**)[b]	−0.24 (d, 1H, $^2J_{HH}$ = 9.0 Hz)	5.59 (s, 5H)
	−0.73 (d, 1H, $^2J_{HH}$ = 9.2 Hz)	1.71 (s, 15H)
	−1.58 (br, 1H)	
$Cp^*CpZr(\mu\text{-}H)_3(Al^iBu_2)_3(\mu\text{-}Cl)_2$ (**3b**)[b]	−0.18 (t, 1H, J_{HH} = 6.7 Hz)	5.55 (s, 5H)
	−1.52 (d, 1H, $^2J_{HH}$ = 5.7 Hz)	1.63 (s, 15H)
$Cp^*_2HfHCl{*}TIBA$[c]	13.17 (s, 1H)	1.89 (s, 30H)

[a]Recorded at −40 °C in C_7D_8. [b]Recorded at −35 °C in C_7D_8. [c]Recorded at room temperature in C_6D_6.

for the mixture formed from the reaction of **3** and TIBA is shown in Figure 3. Solution NMR data for reaction products from **1** and **2** are given in the Supporting Information. In all cases, the room temperature ^{1}H NMR signals for the bridging hydrides are broad and cooling to ∼−20 °C results in sharp signal characteristics of two Zr−H−Al species in solution. These data are consistent with the formation of **1a**−**3a** as the major products in these reactions, while **1b**−**3b** appear at low temperatures.

Unlike **1**−**3**, $Cp^*_2ZrCl_2$ (Cp^* = pentamethylcyclopentadienyl, **4**) does not react with TIBA to form Zr−H−Al species. The ^{1}H NMR spectrum of **4**/TIBA (Al/Zr = 12:1) contains signals at 1.77 ppm assigned to unreacted starting materials and 1.82 ppm assigned to an adduct of $Cp^*_2ZrCl_2$ with TIBA. Signals for $Cp^*_2Zr(^i Bu)Cl$, $Cp^*_2Zr(^i Bu)_2$, $Cp^*_2Zr(^i Bu)H$, or $Cp^*_2ZrH_2$ are not present in this mixture. In contrast, $Cp^*_2HfCl_2$ reacts with

https://doi.org/10.1021/acs.organomet.2c00067
Organometallics 2022, 41, 892−899

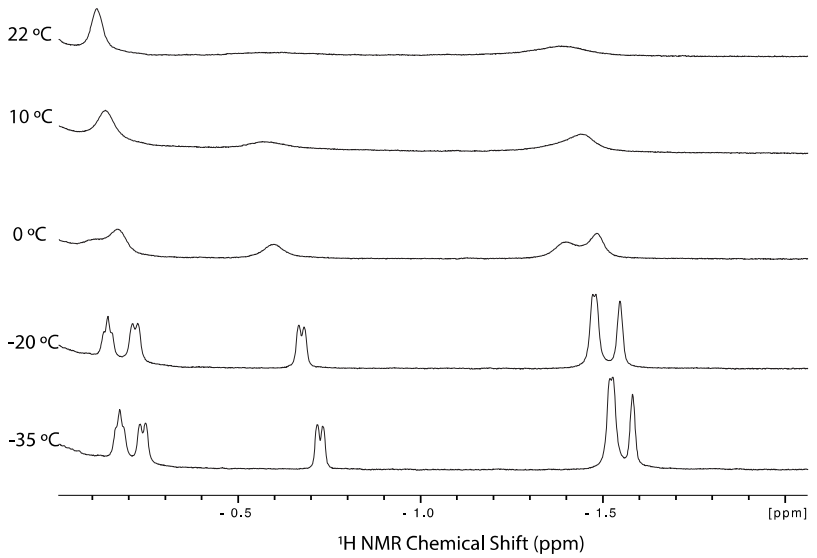

Figure 3. Variable temperature ^{1}H NMR spectra of the hydride region for the reaction of **3** with TIBA (Al/Zr = 12:1) in C_7D_8.

TIBA (Al/Zr = 12:1) to form Cp^*_2HfHCl in ∼15% yield determined by ^{1}H NMR integration. This mixture is stable for days at room temperature and does not progress to form greater amounts of Cp^*_2HfHCl. The signal for Hf−H appears at 13.17 ppm. This signal is shifted 0.49 ppm higher in frequency relative to that of Cp^*_2HfHCl,[22] suggesting that TIBA forms an adduct, but not a bridging hydride, with Cp^*_2HfHCl in this mixture.

A plausible reaction cascade to form **1a** and **1b** is shown in Figure 4. Zr−Cl/Al−^{i}Bu exchange forms the unobserved

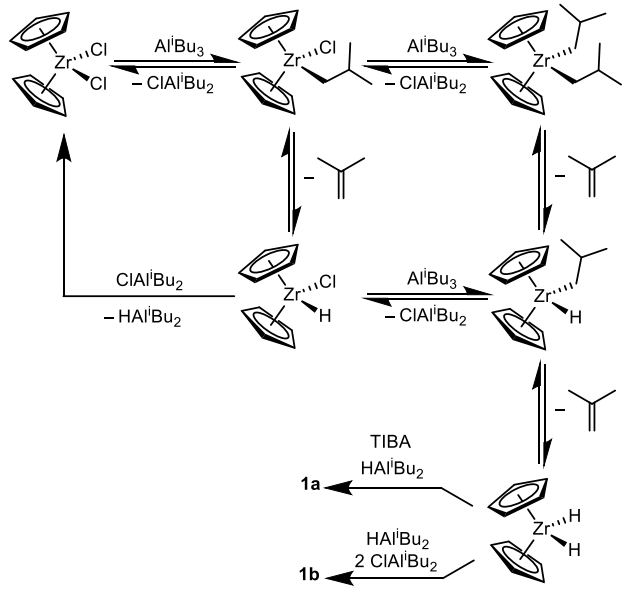

Figure 4. Reactions involved in the formation of **1a** and **1b**.

$Cp_2Zr(^iBu)Cl$ that undergoes β-hydride elimination to form Cp_2ZrHCl and isobutene. Repetition of this sequence ultimately generates Cp_2ZrH_2, which may be trapped by HAl^{i}Bu$_2$ and TIBA to form **1a** or by HAl^{i}Bu$_2$ and ClAl^{i}Bu$_2$ to form **1b**. Alternatively, $Cp_2Zr(^iBu)Cl$ could react with additional TIBA to form $Cp_2Zr(^iBu)_2$, which would similarly undergo β-hydride elimination to form Cp_2ZrH_2. Though HAl^{i}Bu$_2$ is often present in commercial TIBA, reactions of Cp_2ZrHCl or Cp_2ZrH_2 with ClAl^{i}Bu$_2$ could also result in formation of HAl^{i}Bu$_2$, suggesting that the presence or absence of HAl^{i}Bu$_2$ in the TIBA feed would have minimal impact on reactions shown in Figure 4.

The reactions shown in Figure 4 are expected based on the reactivity of AlR_3 with metallocene dichlorides. The Zr−^{i}Bu fragment is known to undergo reversible β-H elimination/re-insertion reactions under mild conditions.[23] In the presence of excess TIBA and HAl^{i}Bu$_2$, the insertion of isobutene into a Zr−H is suppressed and formation of either **1**−**3a** or **1**−**3b** is favored.

***Ansa*-Metallocenes.** *Rac*-(2-Methyl-SBI)$ZrCl_2$ (**6**) and *rac*-(EBI)$ZrCl_2$ (**7**) react with TIBA to form organometallics, and, in some cases, hydrides derived from Zr−^{i}Bu. Relevant ^{1}H and ^{13}C NMR data for the products formed in these reactions are summarized in Table 2.

A C_6D_6 slurry of *rac*-(2-methyl-SBI)$ZrCl_2$ (**6**) reacts with 12 equiv of TIBA to immediately dissolve suspended **6** to form an orange solution containing C_s symmetric *rac*-(2-methyl-SBI)-$Zr(CH_2CH(CH_3)_2)Cl$ (**6a**) as the only identifiable product, eq 2. Several minor species also form in this reaction, and over the

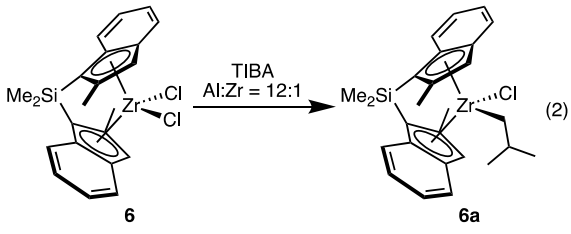

course of ∼24 h, at 25 °C, a greenish brown solution evolves. However, only **6a** is observed by NMR in solution, and no other Zr−R or Zr−H species evolve in this mixture. The ^{1}H NMR spectrum of **6a** at 25 °C contains two doublet of doublets at −0.89 (J_{HH} = 13.5, 4.8 Hz) and −0.37 (J_{HH} = 13.5, 8.0 Hz) ppm assigned to Zr−CH_2. The connectivity of the Zr−^{i}Bu fragment was confirmed by ^{1}H−^{1}H gCOSY NMR experiments (Figure S28). ^{1}H−^{13}C HSQC experiments, Figure S29, show that these ^{1}H signals assigned to Zr−CH_2 correlate with a ^{13}C signal at 81.5 ppm, which is at a similar chemical shift as other Zr−^{i}Bu-containing organometallics.

https://doi.org/10.1021/acs.organomet.2c00067
Organometallics 2022, 41, 892−899

Table 2. Relevant ^{1}H and ^{13}C NMR Data for Products Formed in Reactions of 6−7 with 12 equiv TIBA[a]

	Zr−R (R = ^{i}Bu or H)	CpH[b]
rac-(2-methyl-SBI)Zr($CH_2CH(CH_3)_2$)Cl (**6a**)	−0.89 (dd, 1H, J_{HH} = 13.5, 4.8 Hz) −0.37 (dd, 1H, J_{HH} = 13.5, 8.0 Hz) 0.86 (d, 6H, $^2J_{HH}$ = 7.1 Hz) 1.82 (m, 1H)	6.81 (s, 1H) 6.92 (s, 1H)
rac-(EBI)Zr($CH_2CH(CH_3)_2$)Cl (**7a**)	−0.80 (dd, 1H, J_{HH} = 12.6, 5.8 Hz) −0.37 (dd, 1H, J_{HH} = 12.9, 8.0 Hz) 0.74 (d, 3H, J_{HH} = 5.8 Hz) 0.73 (d, 3H, J_{HH} = 5.6 Hz) 1.92 (from COSY, 1H) ^{13}C (HSQC): 85.4 (Zr−CH_2)	5.48 (d, 1H, J_{HH} = 3.4 Hz) 5.84 (d, 1H, J_{HH} = 3.3 Hz) 6.52 (d, 1H, J_{HH} = 2.7 Hz) 6.57 (d, 1H, J_{HH} = 3.4 Hz)
rac-(EBI)Zr(μ-Cl)(μ-CH_2CH_2)Al^{i}Bu$_2$ (**7b**)	−2.03 (ddd, 1H, J_{HH} = 12.7, 8.5, 3.8 Hz) −0.73 (ddd, 1H, J_{HH} = 12.7, 8.5, 8.5 Hz) 0.45 (from COSY, 1H) 1.23 (from COSY, 1H) ^{13}C (HSQC): 55.5 (Zr−CH_2) 5.5 (Al−CH_2)	4.95 (d, 1H, J_{HH} = 3.2 Hz) 5.59 (d, 1H, J_{HH} = 3.2 Hz) 5.54 (d, 1H, J_{HH} = 3.3 Hz) 5.89 (d, 1H, J_{HH} = 3.3 Hz)
rac-(EBI)Zr(μ-H)(μ-CH_2CH_2)Al^{i}Bu$_2$ (**7c**)	−2.62 (br s, 1H, Zr− H−Al) −2.12 (m, 1H) −1.58 (m, 1H) 0.14 (m, 1H) 1.17 (from COSY, 1H) ^{13}C (HSQC): 53.4 (Zr−CH_2) 4.7 (Al−CH_2)	4.41, 5.25, 5.76, 6.03[c]
rac-(EBI)ZrH(μ-H)$_2$Al^{i}Bu$_2$ (**7d**)	−1.77 (d, 1H, J_{HH} = 6.3 Hz) −1.44 (br s, 1H) −0.22 (from COSY, 1H)	5.11, 5.45, 6.51, 6.52[c]
rac-(EBI)ZrH(μ-H)$_2$[μ-H(AliBu$_2$)$_2$] (**7e**)	−0.93 (br s) −0.24 (d, 1H, J_{HH} = 9.2 Hz) −0.07 (from COSY, 1H)	[d]5.21, 5.37, 5.74, 5.81, 5.87, 5.91, 5.96, 6.00
rac-(EBI)ZrH(μ-H)$_2$[μ-Cl(AliBu$_2$)$_2$] (**7f**)	−1.39 (br s, 1H) −1.26 (d, 1H, J_{HH} = 9.2 Hz) 0.86 (from COSY, 1H)	

[a]Recorded at 25 °C in C_6D_6. [b]Other ligand resonances, when assignable, are given in the Supporting Information. [c]Appear as broad doublets, not possible to resolve *J*-couplings from these data. [d]A total of eight signals is attributed to **7e** and **7f**.

The chemistry *rac*-(EBI)$ZrCl_2$ (**7**) with 12 equiv TIBA is significantly more complicated. The alkyl/hydride region of the ^{1}H NMR spectra of this mixture over 40 h is shown in Figure 5a−e, and a reaction scheme showing the products evolved in this reaction with relevant NMR data is shown in Figure 5f. Monitoring this mixture over 10 days at room temperature does not contain signals in addition to those shown in Figure 5e.

Similar to the reaction of **6** and TIBA, undissolved **7** reacts rapidly with TIBA to form an orange solution. After ∼10 min at 25 °C, the ^{1}H NMR spectrum contains the C_s symmetric *rac*-(EBI)Zr($CH_2CH(CH_3)_2$)Cl (**7a**, major, 95%) and *rac*-(EBI)Zr(μ-Cl)(μ-CH_2CH_2)Al^{i}Bu$_2$ (**7b**, minor, 5%). **7b** contains a characteristic coupling pattern for the μ-CH_2CH_2 signals at −2.03 (ddd, J_{HH} = 12.7, 8.5, and 3.8 Hz) and −0.73 ppm (ddd, J_{HH} = 12.7, 8.5, and 8.5 Hz). The other two signals in the μ-CH_2CH_2 fragment are obscured by signals from excess TIBA but are observable with ^{1}H−^{1}H COSY experiments at 0.45 and 1.23 ppm. These sets of protons correlate with ^{13}C NMR signals at 5.5 (Al−CH_2) and 55.5 ppm (Zr−CH_2) in ^{1}H−^{13}C HSQC experiments.

Over the course of 3 h, the signals for **7a** and **7b** decay and signals for *rac*-(EBI)Zr(μ-H)(μ-CH_2CH_2)Al^{i}Bu$_2$ (**7c**) and *rac*-(EBI)ZrH(μ-H)$_2$Al^{i}Bu$_2$ (**7d**) appear. Signals assigned to *rac*-(EBI)ZrH(μ-H)$_2$[μ-H(AliBu$_2$)$_2$] (**7e**) and *rac*-(EBI)ZrH(μ-H)$_2$[μ-Cl(AliBu$_2$)$_2$] (**7f**) appear in the ^{1}H NMR spectra of this mixture after aging 16 h.[24] As this reaction progresses toward the sets of ^{1}H NMR signals shown in Figure 5e, a signal for isobutane (0.86 ppm, d, J_{HH} = 7.1 Hz) increases in intensity. In addition, a signal in the ^{13}C NMR spectrum at 9.7 ppm assigned to (MeAl^{i}Bu$_2$)$_n$ appears.[25] **7** does not react to form products that result from a metal-to-benzo-ring hydride transfer.[26]

Formation of **7b** and **7c** can be rationalized by the reaction steps shown in Scheme 1, which also accounts for the formation of isobutane and (MeAl^{i}Bu$_2$)$_n$ present in solution. Alkylation of **7a** with TIBA forms *rac*-(EBI)Zr(^{i}Bu)$_2$, and β-abstraction generates the key unobserved Zr(II) intermediate *rac*-(EBI)Zr(isobutene)(ClAl^{i}Bu$_2$) and isobutane.[27] Carboalumination of *rac*-(EBI)Zr(isobutene)(ClAl^{i}Bu$_2$) forms the substituted *rac*-(EBI)Zr(μ-Cl)(μ-$CH_2C(CH_3)_2$)Al^{i}Bu$_2$. Subsequent β-methyl elimination,[28] Al−R/Zr−Me alkyl exchange, and hydrozirconation steps ultimately form **7b**. Al−H/Zr−Cl exchange with HAl^{i}Bu$_2$ present in solution likely forms **7c**. These steps are apparently quite fast; intermediates or possible products expected from dissociation of aluminumalkyl intermediates with free TIBA or HAl^{i}Bu$_2$ are not observed in solution. These steps may also be accelerated by Lewis acidic chloroalkylaluminum species in solution that may form transient ion pairs.[29]

https://doi.org/10.1021/acs.organomet.2c00067
Organometallics 2022, 41, 892−899

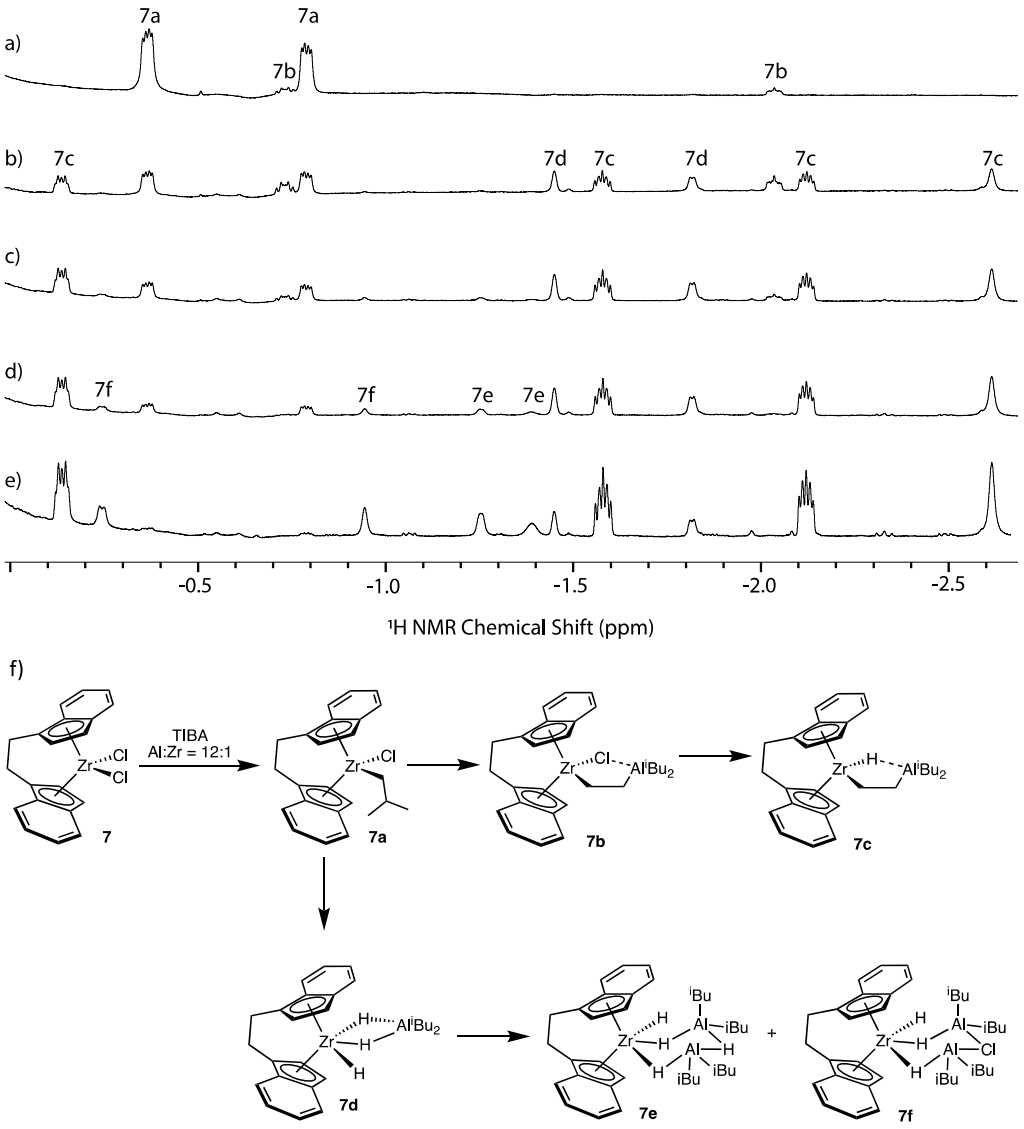

Figure 5. Excerpt of the ^{1}H NMR spectra of the reaction of 7 with TIBA (Al/Zr = 12:1) in C_6D_6 at 25 °C; ∼10 min after mixing (a); 3 h after mixing (b); 9 h after mixing (c); 16 h after mixing (d); and 40 h after mixing (e). Evolution of products formed in this mixture (f).

Scheme 1. Plausible Reaction Steps Resulting in the Formation of 7b and 7c

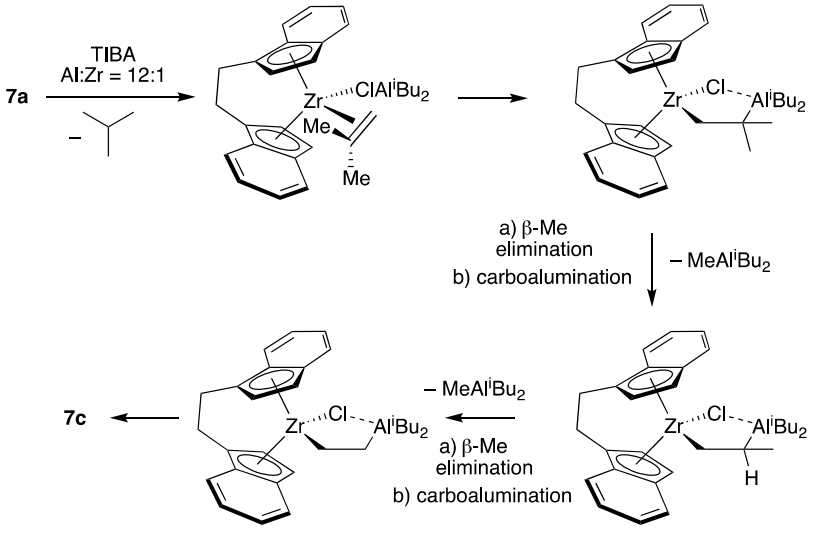

https://doi.org/10.1021/acs.organomet.2c00067
Organometallics 2022, 41, 892−899

To the best of our knowledge, this reactivity has not been observed with Al^iBu_3 and **7**. However, there is precedent for formation of Zr(II) and similar reaction products in carboalumination reactions. For example, computational studies of $Cp_2Zr(ethylene)$ and $ClAlEt_2$ show that formation of $Cp_2Zr(\mu\text{-}Cl)(\mu\text{-}CH_2CH_2)AlEt_2$ is barrierless and exothermic (ΔG_{298} = −13.6 kcal mol^{-1}), though formation of $Cp_2Zr(\mu\text{-}H)(\mu\text{-}CH_2CH_2)AlEt_2$ is more favorable thermodynamically (ΔG_{298} = −27.6 kcal mol^{-1}).[30] Additionally, reactions of $CpCp'ZrCl_2$ (Cp′ = 1-neomenthyl-4,5,6,7-tetrahydroindenyl) and $AlEt_3$ form similar $CpCp'Zr(\mu\text{-}H)(\mu\text{-}CH_2CH_2)AlEt_2$ products and were proposed to form through Zr(II) intermediates.[31] The formation of **7b** and **7c** as major products in the reaction of **7** and TIBA may account for the poor reactivity of this mixture in carboalumination of 1-octene.[24]

The formation of **7d**, **7e**, and **7f** is more straightforward and related to the results obtained for unbridged metallocenes. Exhaustive Al−^{i}Bu/Zr−Cl and β-hydride elimination from **7a** ultimately form these products. Though **7b** and, subsequently, **7c**, form rapidly in this mixture, there is an appreciable amount of these Zr−H species that evolve over the course of several hours. This result suggests that β-hydride elimination from **7a** is on a similar, but slower, timescale than formation of the Zr(II) intermediate shown in Scheme 1.

CONCLUSIONS

Sterically open unbridged metallocenes react with TIBA to form mixtures of bridging hydrides. From the compounds studied here, there were no obvious trends relating sterics of the metallocene to formation of **1**−**3a** or **1**−**3b**. The most apparent similarity in reactions of TIBA with *ansa*-metallocenes or unbridged metallocenes is intermediacy of Zr−^{i}Bu species, which are not observable in unbridged metallocenes but are observable in reactions of **6** or **7** with TIBA. In the former case, rapid β-hydride elimination to form hydrides dominates the reaction chemistry to form **1**−**3a** and **1**−**3b**. Of the two *ansa*-metallocenes studied here, only **7** shows this reactivity pattern, though the formation of hydrides in this mixture is somewhat slower than reaction steps involving Zr(II) to form **7b**.

This study adds to the complex and promiscuous reaction chemistry encountered in mixtures of metallocenes and alkylaluminum reagents. As mentioned above, the addition of TIBA to mixtures of metallocenes and MAO can have advantages in polymerization reaction. The formation of hydrides in reactions of TIBA and metallocenes is undoubtedly related to this behavior, but this study shows that these reactions can be significantly more complex, particularly in the absence of activators that form cationic species.

EXPERIMENTAL METHODS

General Comments. All manipulations were performed under an inert atmosphere of dinitrogen or argon using standard Schlenk or glovebox techniques. Benzene-d_6 and toluene-d_8 were purchased from Cambridge Isotope Laboratories, dried over sodium/benzophenone, degassed by three freeze−pump−thaw cycles, distilled under vacuum, and stored in an inert atmosphere glovebox. Triisobutylaluminum was purchased from Sigma-Aldrich. All other commercially available reagents were used as received without any purification. $Cp^*CpZrCl_2$ was synthesized using published procedures.[32] *Ansa*-metallocenes shown in Figure 3 were provided by Chevron Phillips Chemical.

General Procedure for TIBA Activation of Metallocenes. A Teflon valved NMR tube was loaded with metallocene dichloride (0.03 mmol) and 0.4 mL of C_6D_6 in an inert atmosphere glovebox. TIBA (0.09 mL, 0.36 mmol, 12 equiv) was added using a syringe to the NMR tube, and the valve was sealed. Solution NMR experiments were recorded at ambient temperature. Species requiring low temperature NMR measurements were prepared using an identical procedure but using toluene-d_8 as solvent. Many of the *ansa*-metallocenes shown in Figure 3 are sparingly soluble in C_6D_6 at room temperature, but TIBA results in clear orange solutions after brief (∼1 min) agitation of the NMR tube.

Solution NMR spectra were acquired on a Bruker Avance 7.05 T (^{1}H = 300 MHz), Bruker Avance 14.1 T (^{1}H = 600 MHz), or Bruker Avance III 16.5 T (^{1}H = 700 MHz) NMR spectrometer. ^{1}H NMR spectra were referenced to the residual natural abundance ^{1}H NMR signal from the NMR solvent. Assignments to the species formed in solution are listed below. In cases where accurate integration of the ^{1}H NMR spectrum is not possible due to overlapping signals, assignments were made from ^{1}H−^{1}H COSY and/or ^{1}H−^{1}H NOESY experiments. ^{13}C NMR assignments were made using ^{1}H−^{13}C HSQC experiments when assignment of ^{1}H NMR signals was possible.

NMR Data for ***1a****.* ^{1}H NMR (600 MHz, C_7D_8, −40 °C): −2.53 (br, 1H), −1.90 (d, 1H, J_{HH} = 8.0 Hz), −1.22 (d, 1H, $^2J_{HH}$ = 8.2 Hz), 0.34 (from NOESY(Cp)/COSY; Al−CH_2), 1.28 (from COSY; Al−$CH_2CH(CH_3)_2$), 2.10 (from COSY; Al−$CH_2CH(CH_3)_2$), 5.48 (s, 10H). ^{13}C{^{1}H} NMR (600 MHz, C_7D_8, −40 °C): 24.82, 26.07, 27.04, 27.96, 28.59, 29.18, 103.95.

NMR Data for ***1b****.* ^{1}H NMR (600 MHz, C_7D_8, −40 °C): −2.55 (d, 2H, J_{HH} = 7.3 Hz), −1.16 (t, 1H, J_{HH} = 7.4 Hz), 5.46 (s, 10H). ^{13}C{^{1}H} NMR (600 MHz, C_7D_8, −40 °C): 104.91 (Cp). Clear assignments of the TIBA resonances were not possible from the solution NMR data, for the preparation of **1b** from HAl^iBu_2 and **1** see ref 19.

NMR Data for ***2a****.* ^{1}H NMR (600 MHz, C_7D_8, −30 °C): −1.73 (br, 1H), −0.55 (d, 1H, J_{HH} = 9.5 Hz), −0.49 (d, 1H, J_{HH} = 9.1 Hz), 0.32 (from NOESY(Cp)/COSY; Al−CH_2), 0.54 (from NOESY-(Cp)/COSY; Al−CH_2), 1.10 (from COSY; Al−$CH_2CH(CH_3)_2$), 1.12 (from COSY), 2.04 (from COSY; Al−$CH_2CH(CH_3)_2$), 5.48 (s, 10H). ^{13}C{^{1}H} NMR (600 MHz, C_7D_8, −30 °C): 12.56 (CpMe), 102.1 (Cp). 24.83, 26.72, 28.34, 28.60, 102.1 (Cp).

NMR Data for ***2b****.* ^{1}H NMR (600 MHz, C_7D_8, −30 °C): −1.65 (br, 1H), −0.45 (t, 1H, J_{HH} = 6.1 Hz), 5.47 (s, 10H). ^{13}C{^{1}H} NMR (600 MHz, C_7D_8, −30 °C): 102.9 (Cp). Clear assignments of the TIBA resonances were not possible from the solution NMR data, for the preparation of **2b** from HAl^iBu_2 and **2** see ref 19. TIBA resonances were not resolvable from the solution NMR data.

NMR Data for ***3a****.* ^{1}H NMR (600 MHz, C_7D_8, −40 °C): −1.58 (br, 1H), −0.73 (d, 1H, $^2J_{HH}$ = 9.2 Hz), −0.24 (d, 1H, $^2J_{HH}$ = 9.0 Hz), 0.38 (from NOESY(Cp)/COSY; Al−CH_2), 1.47 (from COSY; Al−$CH_2CH(CH_3)_2$), 1.95 (from COSY; Al−$CH_2CH(CH_3)_2$), 1.71 (s, 15H), 2.11 (m, 3H), 2.23 (m, 2H), 5.59 (s, 5H). ^{13}C{^{1}H} NMR (600 MHz, C_7D_8, −40 °C): 12.56 (CpMe). TIBA resonances were not resolvable from the solution NMR data.

NMR Data for ***3b****.* ^{1}H NMR (600 MHz, C_7D_8, −40 °C): −1.52 (d, 1H, $^2J_{HH}$ = 5.7 Hz), −0.18 (t, 1H, J_{HH} = 6.7 Hz), 0.53 (from NOESY(Cp)/COSY; Al−CH_2), 1.18 (from COSY; Al−$CH_2CH(CH_3)_2$), 2.14 (from COSY; Al−$CH_2CH(CH_3)_2$), 5.55 (s, 5H). ^{13}C{^{1}H} NMR (600 MHz, C_7D_8, −40 °C): 12.56 (CpMe), 118.18 (Cp). TIBA resonances were not resolvable from the solution NMR data.

NMR Data for ***6a****.* ^{1}H NMR (600 MHz, C_6D_6, 25 °C): −0.89 (dd, 1H, J_{HH} = 13.5, 4.8 Hz), −0.37 (dd, 1H, J_{HH} = 13.5, 8.0 Hz), 0.64 (s, 3H, SiMe), 0.69 (s, 3H, SiMe), 0.86 (d, 6H, $^2J_{HH}$ = 7.1 Hz), 1.69 (s, 3H, CH_3), 1.82 (m, 1H), 1.97 (s, 3H, CH_3), 6.66 (m, 1H), 6.73 (m, 1H), 6.81 (s, 1H), 6.92 (s, 1H), 7.17 (d, 1H, $^3J_{HH}$ = 9.4 Hz), 7.26 (d, 1H, $^3J_{HH}$ = 8.6 Hz), 7.31 (d, 1H, $^3J_{HH}$ = 8.1 Hz), 7.46 (d, 1H, $^3J_{HH}$ = 8.1 Hz). ^{13}C{^{1}H} NMR (600 MHz, C_6D_6, 25 °C): 1.77 (SiMe), 1.83 (SiMe), 17.5 (CH_3), 17.9 (CH_3), 24.6 ($ZrCH_2CH(CH_3)_2$), 33.1 ($ZrCH_2CH(CH_3)_2$), 81.5 ($ZrCH_2CH(CH_3)_2$), 110.6, 116.9, 117.4, 124.6, 124.7, 125.0, 125.4, 125.7, 126.2, 125.8, 126.9.

As shown in Figure 5 of the manuscript, mixtures of **7** and TIBA result in several organozirconium species. Due to this complexity, only

https://doi.org/10.1021/acs.organomet.2c00067
Organometallics 2022, 41, 892−899

the Zr−R, hydride and CpH signals are assigned for **7b** and **7c**. The NMR data for **7d**, **7e**, and **7f** are given in Table 2 of the manuscript.

*NMR Data for **7a**.* ^{1}H NMR (600 MHz, C_6D_6, 25 °C): −0.80 (dd, 1H, J_{HH} = 12.6, 5.8 Hz), −0.37 (dd, 1H, J_{HH} = 12.9, 8.0 Hz), 0.74 (d, 3H, $^{2}J_{HH}$ = 5.8 Hz), 0.73 (d, 3H, $^{2}J_{HH}$ = 5.6 Hz), 1.92 (from COSY, CH), 5.48 (d, 1H, $^{3}J_{HH}$ = 3.4 Hz), 5.84 (d, 1H, $^{3}J_{HH}$ = 3.3 Hz), 6.52 (br d, 1H, $^{3}J_{HH}$ = 2.7 Hz), 6.57 (d, 1H, $^{3}J_{HH}$ = 3.4 Hz), 6.85 (m, 1H), 6.92 (m, 1H), 7.04 (m, 1H), 7.07 (m, 1H), 7.32 (d, 1H, $^{3}J_{HH}$ = 8.4 Hz), 7.35 (d, 1H, $^{3}J_{HH}$ = 9.0 Hz), 7.39 (d, 1H, $^{3}J_{HH}$ = 8.4 Hz), 7.43 (d, 1H, $^{3}J_{HH}$ = 8.8 Hz). $^{13}C\{^{1}H\}$ NMR (600 MHz, C_6D_6, 25 °C): 26.7 ($ZrCH_2CH(CH_3)_2$), 28.1 ($ZrCH_2CH(CH_3)_2$), 26.5 ($ZrCH_2CH(CH_3)_2$), 85.4 ($ZrCH_2CH(CH_3)_2$), 105.2 (Cp), 107.5 (Cp), 112.7 (Cp), 114.6 (Cp), 123.9, 125.9, 126.5, 126.0, 126.6, 126.7.

*NMR Data for **7b**.* ^{1}H NMR (600 MHz, C_6D_6, 25 °C): −2.03 (ddd, 1H, J_{HH} = 12.7, 8.5, 3.8 Hz), −0.73 (ddd, 1H, J_{HH} = 12.7, 8.5, 8.5 Hz), 0.45 (from COSY, 1H), 1.23 (from COSY, 1H), 4.95 (d, 1H, $^{3}J_{HH}$ = 3.2 Hz), 5.59 (br d, 1H, $^{3}J_{HH}$ = 3.2 Hz), 5.54 (d, 1H, $^{3}J_{HH}$ = 3.3 Hz), 5.89 (d, 1H, $^{3}J_{HH}$ = 3.3 Hz). $^{13}C\{^{1}H\}$ NMR (600 MHz, C_6D_6, 25 °C): 6.4 ($Zr(m\text{-}CH_2CH_2)Al^{i}Bu_2$), 55.6 ($Zr(m\text{-}CH_2CH_2)Al^{i}Bu_2$), 95.1, 100.1, 110.2, 114.3.

*NMR Data for **7c**.* ^{1}H NMR (600 MHz, C_6D_6, 25 °C): −2.62 (br s, 1H, Zr−H−Al), −2.12 (m, 1H), −1.58 (m, 1H), 0.14 (m, 1H), 1.17 (from COSY, 1H), 4.41 (br, 1H), 5.25 (br, 1H), 5.76 (br, 1H), 6.03 (br, 1H). $^{13}C\{^{1}H\}$ NMR (600 MHz, C_6D_6, 25 °C): 4.55($Zr(m\text{-}CH_2CH_2)Al^{i}Bu_2$), 53.3 ($Zr(m\text{-}CH_2CH_2)Al^{i}Bu_2$), 90.6, 91.4, 108.6, 112.4.

■ ASSOCIATED CONTENT

Supporting Information

The Supporting Information is available free of charge at https://pubs.acs.org/doi/10.1021/acs.organomet.2c00067.

Experimental methods, solid-state NMR spectra, and solution NMR spectra of polymers (PDF)

■ AUTHOR INFORMATION

Corresponding Authors

Graham Lief − *Bartlesville Research and Technology Center, Chevron Phillips Chemical, Bartlesville, Oklahoma 74003, United States*; Email: liefgr@cpchem.com

Matthew P. Conley − *Department of Chemistry, University of California, Riverside, Riverside, California 92521, United States*; orcid.org/0000-0001-8593-5814; Email: matthew.conley@ucr.edu

Authors

Damien B. Culver − *Department of Chemistry, University of California, Riverside, Riverside, California 92521, United States*

Jamesjohn Corieri − *Department of Chemistry, University of California, Riverside, Riverside, California 92521, United States*

Complete contact information is available at: https://pubs.acs.org/10.1021/acs.organomet.2c00067

Author Contributions

The manuscript was written through contributions of all authors.

Notes

The authors declare no competing financial interest.

■ ACKNOWLEDGMENTS

M.P.C. is a member of the UCR Center for Catalysis. This work was supported by Chevron Phillips Chemical. Portions of NMR spectroscopy described in this manuscript were supported by the National Science Foundation (CHE-2101582).

■ REFERENCES

(1) Dioumaev, V. K.; Harrod, J. F. Nature of the Species Present in the Zirconocene Dichloride−Butyllithium Reaction Mixture. *Organometallics* **1997**, *16*, 1452−1464.

(2) (a) Negishi, E.-I.; Takahashi, T. Patterns of Stoichiometric and Catalytic Reactions of Organozirconium and Related Complexes of Synthetic Interest. *Acc. Chem. Res.* **1994**, *27*, 124−130. (b) Buchwald, S. L.; Nielsen, R. B. Group 4 metal complexes of benzynes, cycloalkynes, acyclic alkynes, and alkenes. *Chem. Rev.* **1988**, *88*, 1047−1058. (c) Beaumier, E. P.; Pearce, A. J.; See, X. Y.; Tonks, I. A. Modern applications of low-valent early transition metals in synthesis and catalysis. *Nat. Rev. Chem.* **2019**, *3*, 15−34.

(3) Negishi, E.; Van Horn, D. E.; Yoshida, T. Controlled carbometalation. 20. Carbometalation reaction of alkynes with organoalene-zirconocene derivatives as a route to stereo-and regiodefined trisubstituted alkenes. *J. Am. Chem. Soc.* **1985**, *107*, 6639−6647.

(4) Xu, S.; Negishi, E.-i. Zirconium-Catalyzed Asymmetric Carboalumination of Unactivated Terminal Alkenes. *Acc. Chem. Res.* **2016**, *49*, 2158−2168.

(5) Long, W. P.; Breslow, D. S. Polymerization of Ethylene with Bis-(cyclopentadienyl)-titanium Dichloride and Diethylaluminum Chloride. *J. Am. Chem. Soc.* **1960**, *82*, 1953−1957.

(6) (a) Kaminskly, W.; Vollmer, H.-J. Kernresonanzspektroskopische Untersuchungen an den Systemen Dicyclopentadienylzirkon(IV) und Organoaluminium. *Just. Lieb. Ann. Chem.* **1975**, *1975*, 438−448. (b) Kaminsky, W.; Kopf, J.; Thirase, G. Notiz über die Röntgenstrukturanalyse von Al,Zr-μ-Chloro-1-[bis(cyclopentadienyl)-zirkonio(IV)]-2,2-bis(diäthylaluminio)äthan. *Just. Lieb. Ann. Chem.* **1974**, *1974*, 1531−1533. (c) Kaminsky, W.; Kopf, J. r.; Sinn, H. r.; Vollmer, H.-J. r. Extreme Bond Angle Distortion in Organozirconium Compounds Active Toward Ethylene. *Angew. Chem., Int. Ed.* **1976**, *15*, 629−630.

(7) Siedle, A. R.; Newmark, R. A.; Schroepfer, J. N.; Lyon, P. A. Solvolysis of dimethylzirconocene by trialkylaluminum compounds. *Organometallics* **1991**, *10*, 400−404.

(8) Kaminsky, W. The discovery of metallocene catalysts and their present state of the art. *J. Polym. Sci., Part A: Gen. Pap.* **2004**, *42*, 3911−3921.

(9) (a) Sishta, C.; Hathorn, R. M.; Marks, T. J. Group 4 metallocene-alumoxane olefin polymerization catalysts. CPMAS-NMR spectroscopic observation of cation-like zirconocene alkyls. *J. Am. Chem. Soc.* **1992**, *114*, 1112−1114. (b) Bochmann, M. The Chemistry of Catalyst Activation: The Case of Group 4 Polymerization Catalysts. *Organometallics* **2010**, *29*, 4711−4740.

(10) (a) Ehm, C.; Cipullo, R.; Budzelaar, P. H. M.; Busico, V. Role (s) of TMA in polymerization. *Dalton Trans.* **2016**, *45*, 6847. (b) Ghiotto, F.; Pateraki, C.; Severn, J. R.; Friederichs, N.; Bochmann, M. Rapid evaluation of catalysts and MAO activators by kinetics: what controls polymer molecular weight and activity in metallocene/MAO catalysts? *Dalton Trans.* **2013**, *42*, 9040−9048. (c) Babushkin, D. E.; Semikolenova, N. V.; Zakharov, V. A.; Talsi, E. P. Mechanism of dimethylzirconocene activation with methylaluminoxane: NMR monitoring of intermediates at high Al/Zr ratios. *Macromol. Chem. Phys.* **2000**, *201*, 558−567. (d) Petros, R. A.; Norton, J. R. Effectiveness in Catalyzing Carboalumination Can Be Inferred from the Rate of Dissociation of M/Al Dimers. *Organometallics* **2004**, *23*, 5105−5107.

(11) Bochmann, M.; Lancaster, S. J. Monomer−Dimer Equilibria in Homo- and Heterodinuclear Cationic Alkylzirconium Complexes and Their Role in Polymerization Catalysis. *Angew. Chem. Int. Ed.* **1994**, *33*, 1634−1637.

(12) Camara, J. M.; Petros, R. A.; Norton, J. R. Zirconium-Catalyzed Carboalumination of α-Olefins and Chain Growth of Aluminum Alkyls: Kinetics and Mechanism. *J. Am. Chem. Soc.* **2011**, *133*, 5263−5273.

(13) (a) Chen, E. Y.-X.; Marks, T. J. Cocatalysts for Metal-Catalyzed Olefin Polymerization: Activators, Activation Processes, and Structure Activity Relationships. *Chem. Rev.* **2000**, *100*, 1391−1434. (b) Coates, G. W.; Hustad, P. D.; Reinartz, S. Catalysts for the Living Insertion Polymerization of Alkenes: Access to New Polyolefin Architectures Using Ziegler−Natta Chemistry. *Angew. Chem., Int. Ed.* **2002**, *41*, 2236−2257.
(14) Brintzinger, H.-H.; Ruchatz, D.; Fink, G. Polymeryl Exchange between ansa-Zirconocene Catalysts for Norbornene−Ethene Copolymerization and Aluminum or Zinc Alkyls. *Macromolecules* **2005**, *38*, 2056−2063.
(15) Bryliakov, K. P.; Semikolenova, N. V.; Panchenko, V. N.; Zakharov, V. A.; Brintzinger, H. H.; Talsi, E. P. Activation of rac-Me2Si(ind)2ZrCl2 by Methylalumoxane Modified by Aluminum Alkyls: An EPR Spin-Probe, 1H NMR, and Polymerization Study. *Macromol. Chem. Phys.* **2006**, *207*, 327−335.
(16) (a) Babushkin, D. E.; Brintzinger, H. H. Modification of Methylaluminoxane-Activated ansa-Zirconocene Catalysts with Triisobutylaluminum—Transformations of Reactive Cations Studied by NMR Spectroscopy. *Chem.—Eur. J.* **2007**, *13*, 5294−5299. (b) Babushkin, D. E.; Panchenko, V. N.; Timofeeva, M. N.; Zakharov, V. A.; Brintzinger, H. H. Novel Zirconocene Hydride Complexes in Homogeneous and in SiO2-Supported Olefin-Polymerization Catalysts Modified with Diisobutylaluminum Hydride or Triisobutylaluminum. *Macromol. Chem. Phys.* **2008**, *209*, 1210−1219.
(17) Kanbur, U.; Zang, G.; Paterson, A. L.; Chatterjee, P.; Hackler, R. A.; Delferro, M.; Slowing, I. I.; Perras, F. A.; Sun, P.; Sadow, A. D. Catalytic carbon-carbon bond cleavage and carbon-element bond formation give new life for polyolefins as biodegradable surfactants. *Chem* **2021**, *7*, 1347−1362.
(18) Culver, D. B.; Dorn, R. W.; Venkatesh, A.; Meeprasert, J.; Rossini, A. J.; Pidko, E. A.; Lipton, A. S.; Lief, G. R.; Conley, M. P. Active Sites in a Heterogeneous Organometallic Catalyst for the Polymerization of Ethylene. *ACS Cent. Sci.* **2021**, *7*, 1225−1231.
(19) Baldwin, S. M.; Bercaw, J. E.; Brintzinger, H. H. Alkylaluminum-Complexed Zirconocene Hydrides: Identification of Hydride-Bridged Species by NMR Spectroscopy. *J. Am. Chem. Soc.* **2008**, *130*, 17423−17433.
(20) (a) Götz, C.; Rau, A.; Luft, G. Ternary metallocene catalyst systems based on metallocene dichlorides and AlBu3i/[PhNMe2H]-[B(C6F5)4]: NMR investigations of the influence of Al/Zr ratios on alkylation and on formation of the precursor of the active metallocene species. *J. Mol. Catal. A: Chem.* **2002**, *184*, 95−110. (b) Parfenova, L. V.; Pechatkina, S. V.; Khalilov, L. M.; Dzhemilev, U. M. Mechanism of Cp2ZrCl2-catalyzed olefin hydroalumination by alkylalanes. *Russ. Chem. Bull.* **2005**, *54*, 316−327.
(21) González-Hernández, R.; Chai, J.; Charles, R.; Pérez-Camacho, O.; Kniajanski, S.; Collins, S. Catalytic System for Homogeneous Ethylene Polymerization Based on Aluminohydride−Zirconocene Complexes. *Organometallics* **2006**, *25*, 5366−5373.
(22) Roddick, D. M.; Fryzuk, M. D.; Seidler, P. F.; Hillhouse, G. L.; Bercaw, J. E. Halide, hydride, alkyl, and dinitrogen complexes of bis(pentamethylcyclopentadienyl)hafnium. *Organometallics* **1985**, *4*, 97−104.
(23) (a) Guo, Z.; Swenson, D. C.; Jordan, R. F. Cationic Zirconium and Hafnium Isobutyl Complexes as Models for Intermediates in Metallocene-Catalyzed Propylene Polymerizations. Detection of an .alpha.-Agostic Interaction in (C5Me5)2Hf(CH2CHMe2)(PMe3)+. *Organometallics* **1994**, *13*, 1424−1432. (b) Pool, J. A.; Bradley, C. A.; Chirik, P. J. A Convenient Method for the Synthesis of Zirconocene Hydrido Chloride, Isobutyl Hydride, and Dihydride Complexes Using tert-Butyl Lithium. *Organometallics* **2002**, *21*, 1271−1277.
(24) Parfenova, L. V.; Kovyazin, P. V.; Nifant'ev, I. E.; Khalilov, L. M.; Dzhemilev, U. M. Role of Zr,Al Hydride Intermediate Structure and Dynamics in Alkene Hydroalumination with XAlBui2 (X = H, Cl, Bui), Catalyzed by Zr η5 Complexes. *Organometallics* **2015**, *34*, 3559−3570.
(25) Hoffmann, E. G. Alkyl group exchange in aluminium trialkyls detected by proton magnetic resonance. *Trans. Faraday Soc.* **1962**, *58*, 642−649.
(26) Bazinet, P.; Tilley, T. D. Octa- and Nonamethylfluorenyl Complexes of Zirconium(IV): Reactive Hydride Derivatives and Reversible Hydrogen Migration between the Metal and the Fluorenyl Ligand. *Organometallics* **2009**, *28*, 2285−2293.
(27) Alkylaluminum reagents are known to reduce Ti(IV) to paramagnetic Ti(II) species, see: Soshnikov, I. E.; Semikolenova, N. V.; Ma, J.; Zhao, K.-Q.; Zakharov, V. A.; Bryliakov, K. P.; Redshaw, C.; Talsi, E. P. Selective Ethylene Trimerization by Titanium Complexes Bearing Phenoxy-Imine Ligands: NMR and EPR Spectroscopic Studies of the Reaction Intermediates. *Organometallics* **2014**, *33*, 1431−1439 Paramagnetic signals from Zr(II) were not present in this mixture.
(28) O'Reilly, M. E.; Dutta, S.; Veige, A. S. β-Alkyl Elimination: Fundamental Principles and Some Applications. *Chem. Rev.* **2016**, *116*, 8105−8145.
(29) *Rac*-(SBI)$ZrCl_2$ reacts with $AliBu_3$/$[CPh_3][B(C_6F_5)_4]$ to form bridging allyl hydride species in solution, see: Bryliakov, K. P.; Talsi, E. P.; Semikolenova, N. V.; Zakharov, V. A.; Brand, J.; Alonso-Moreno, C.; Bochmann, M. Formation and structures of cationic zirconium complexes in ternary systems rac-(SBI)ZrX2/AlBu3i/[CPh3][B(C6F5)4] (X=Cl, Me). *J. Organomet. Chem.* **2007**, *692*, 859−868.
(30) Tyumkina, T. V.; Islamov, D. N.; Parfenova, L. V.; Karchevsky, S. G.; Khalilov, L. M.; Dzhemilev, U. M. Mechanism of Cp2ZrCl2-Catalyzed Olefin Cycloalumination with AlEt3: Quantum Chemical Approach. *Organometallics* **2018**, *37*, 2406−2418.
(31) Parfenova, L. V.; Berestova, T. V.; Molchankina, I. V.; Khalilov, L. M.; Whitby, R. J.; Dzhemilev, U. M.; Dzhemilev, U. M. Stereocontrolled monoalkylation of mixed-ring complex CpCp'ZrCl2 (Cp' = 1-neomenthyl-4,5,6,7-tetrahydroindenyl) by lithium, magnesium and aluminum alkylsStereocontrolled monoalkylation of mixed-ring complex CpCp′ZrCl2 (Cp′ = 1-neomenthyl-4,5,6,7-tetrahydroindenyl) by lithium, magnesium and aluminum alkyls. *J. Organomet. Chem.* **2013**, *726*, 37−45.
(32) Wolczanski, P. T.; Bercaw, J. E. Alkyl and hydride derivatives of (pentamethylcyclopentadienyl)zirconium(IV). *Organometallics* **1982**, *1*, 793−799.

https://doi.org/10.1021/acs.organomet.2c00067
Organometallics 2022, 41, 892−899